Article

Not peer-reviewed version

Hesperetin Inhibits Xanthine Oxidase Activity via Altering the Protein's Secondary Structure and Suppressing Superoxide Anion Generation

Yinying Liu , Qiangqiang Chen , Hanyu Lu , Zhongxiang Fang * , Shengmin Lu *

Posted Date: 25 April 2024

doi: 10.20944/preprints202404.1678.v1

Keywords: Hesperetin; Xanthine oxidase; Inhibition kinetics; Interaction mechanism; Multi-spectroscopy; Molecular docking

 doi:10.20944/preprints202404.1678.v1

Article

Hesperetin Inhibits Xanthine Oxidase Activity via Altering the Protein's Secondary Structure and Suppressing Superoxide Anion Generation

Yinying Liu [1,2], Qianqian Chen [1], Hanyu Lu [1,2], Zhongxiang Fang [2,*] and Shengmin Lu [1,*]

[1] State Key Laboratory for Managing Biotic and Chemical Threats to the Quality and Safety of Agro-products, Zhejiang Key Laboratory of Fruit and Vegetables Postharvest and Processing Technology Research, Ministry of Agriculture and Rural Affairs Key Laboratory of Post-Harvest Handling of Fruits, Institute of Food Science, Zhejiang Academy of Agricultural Science, Hangzhou 310021, China; lyy19970122@gmail.com (Y.L.), chenqianq2023@163.com (Q.C.); luhanyu1234@163.com (H.L)

[2] School of Agriculture, Food and Ecosystem Sciences, The University of Melbourne, Parkville, Vic 3010, Australia

* Correspondence: zhongxiang.fang@unimelb.edu.au (Z.F.); lushengmin@hotmail.com (S.L.); Tel.: 86-571-86417306; 61-3-83445063

Abstract: Hyperuricemia is mainly caused by the overproduction of uric acid (UA) catalyzed from xanthine by xanthine oxidase (XO) in abnormal purine metabolism in human body. There is an increasing demand for developing novel XO inhibitors of plant origins. The inhibition kinetics and type as well as actions of hesperetin against XO were investigated in vitro using multi-spectroscopic methods including UV-Vis absorption, Fourier transform infrared spectroscopy (FT-IR), fluorescence spectroscopy and molecular docking simulation. Results indicated that hesperetin reversibly inhibited XO in a competitive manner with an inhibition constant (K_i) value of (2.15 ± 0.05) × 10^{-6} mol/L. Hesperetin had a higher scavenging rate against O_2^- radical generated by the XO reaction system. The binding of hesperetin to the active site of XO altered the protein's secondary structure as demonstrated by FT-IR and fluorescence spectra. Molecular docking study revealed that hesperetin had highly affinity to XO and the bonding of hesperetin to the molybdopterin (Mo-pt) active center inhibited not only substrate entry, but also prevented oxygen binding to flavin adenine dinucleotide (another active center in XO). Additionally, hydrophobic interactions and hydrogen bonds contributed to the stabilization of the hesperetin-XO complex. The results suggested that hesperetin be a promising natural XO inhibitor to alleviate hyperuricemia and gout.

Keywords: Hesperetin; Xanthine oxidase; Inhibition kinetics; Interaction mechanism; Multi-spectroscopy; Molecular docking

1. Introduction

Hyperuricemia is characterized by the abnormal accumulation of uric acid (UA) in human body, stemming from its overproduction or insufficient excretion. This condition is increasingly recognized as a global health concern (Bao et al., 2022). Multiple studies have indicated that elevated levels of serum UA can lead to crystal formation, contributing to the development of gout and kidney stones. In addition, excessive serum UA is associated with an increased risk of chronic diseases including high blood pressure, heart-related illnesses, insulin resistance and cancer (Dório et al., 2022). Therefore, keeping a balance between the production and excretion of uric acid is essential for human health.

Increasing evidence has suggested that lowering serum UA levels through the inhibition of xanthine oxidase (XO) could be a viable strategy for mitigating hyperuricemia (Chen et al., 2022). XO is a key enzyme involved in purine metabolism that facilitates the conversion of hypoxanthine to

 doi:10.20944/preprints202404.1678.v1

xanthine and further oxidizes xanthine to UA, accompanied by the release of reactive oxygen species (An et al., 2023). Therefore, targeting the inhibition of XO to decrease UA levels presents a promising approach for the prevention and management of hyperuricemia (Dong et al., 2021). Currently, allopurinol and febuxostat are the two primary pharmacological agents clinically approved as xanthine oxidase inhibitors (XOIs). However, they are associated with comorbidities and severe adverse reactions like acute kidney injury and allergic responses (Zhou et al., 2017). Therefore, there is an increasing need to develop effective and safe XOIs derived from medicinal and edible plants for the treatment of hyperuricemia.

Medicinal and food homologous (MFH) plants, which have been widely used in China for thousand of years, are now attracting considerable interest due to their diverse constituents and multifunctional properties as well as their low toxicity (Hou & Jiang, 2013). Secondary metabolites in MFH plants such as alkaloids, polyphenols, polysaccharides, and saponins, have been demonstrated to have anti-hyperuricemia properties by lowering UA levels (Cheng-yuan & Jian-gang, 2023). Hesperetin, a bioactive component in citrus fruit, exhibits antioxidant, anti-cancer, and anti-inflammatory properties (Roohbakhsh et al., 2015; Zare,Sarkati, & Rahaiee, 2021). Consumption of orange juice might contribute to the reduction of hyperuricemia (Haidari et al., 2009; Haidari, Rashidi, & Mohammad-Shahi, 2012), and it had been observed that hesperetin exhibited an inhibitory action against XO (Liu et al., 2016). Hesperetin has also been recognized as an obvious competitive XOI with its IC_{50}=13.63±0.12 μM (Cao et al., 2023). However, there is a notable lack of comprehensive studies investigating how hesperetin inhibits XO and its effectiveness as an antioxidant against XO's reactive by-products. Additionally, the detailed biological mechanism underlying hesperetin's inhibition against XO has yet to be clearly defined.

This study aimed to identify hesperetin's antioxidant properties and XO inhibitive capacity. The antioxidant activities of hesperetin on reactive oxygen species (ROS) and its mechanism of inhibition against XO were investigated by a series of spectroscopy methods and molecular docking. The study would provide theoretical foundation for developing hesperetin as a natural functional food supplement to reduce the risks of hyperuricemia.

2. Materials and Methods

2.1. Chemicals

Xanthine oxidase (EC 1.17.3.2, grade I, from bovine milk, 8.6 U/mg) and xanthine (≥98% in purity) as its substrate were purchased from Shanghai Yuanye Biotechnology Co., Ltd. (Shanghai, China). Hesperetin (97% in purity), allopurinol (98% in purity), nitroblue tetrazolium (NBT), phenazine methosulfate (PMS), β-nicotinamide adenine dinucleotide (β-NADH, reduced) and 2,2-diphenyl-1-picrylhydrazyl (DPPH) were supplied by Macklin Biochemical Co. Ltd. (Shanghai, China). All other reagents and solvents were of analytical grade and ultrapure water prepared by Jielu Pure Water Co. Ltd. (Hangzhou, China) was used in the experiment. Stock solutions were stored at 0-4 °C and all experiments were carried out at room temperature unless otherwise specified.

2.2. Inhibitory Activity of Hesperetin agaist XO

The inhibitory activity of hesperetin agaist XO was carried out according to the method of Zhao et al. (2020) with slight modifications. In brief, various concentrations of hesperetin (100 μL) and fixed concentration of XO (50 μL, 0.04 U/mL) were mixed and incubated at 37 °C for 30 min. The reaction was then initiated by adding xanthine solution (50 μL, 0.5 mM). The absorbance of the mixture was scanned every 15 s for 7 min at 295 nm on a Multiskan FC microplate reader (Thermo Fisher Scientific Inc., Waltham, MA, USA). The blank control was conducted without the tested compound and allopurinol was used as the positive control. Three replicates were performed for each test. The relative inhibition ratio (%) of hesperetin against XO was calculated by Equation (1):

 doi:10.20944/preprints202404.1678.v1

$$Relative\ inhibition\ ratio\ (\%) = \frac{\left(\frac{dA}{dt}\right)_{blank} - \left(\frac{dA}{dt}\right)_{sample}}{\left(\frac{dA}{dt}\right)_{blank}} \times 100 \quad (1)$$

where $\left(\frac{dA}{dt}\right)_{blank}$ and $\left(\frac{dA}{dt}\right)_{sample}$ refer to the enzyme reaction rate of blank group and sample group, respectively. The IC_{50} value, representing the half maximal inhibitory concentration of the tested compound against XO, was calculated using Excel 2013 (Microsoft, Redmond, WA, USA) and GraphPad v9.0 (GraphPad Software, San Diego, CA, USA).

2.3. Inhibition Kinetic and Type of Hesperetin against XO

To determine the reversibility of inhibition, the substrate (xanthine) concentration (0.5 mM) was maintained while the XO concentration was increased (0.01, 0.02, 0.03, 0.04 and 0.05 U/mL). The reaction velocity was measured by adding different concentrations of hesperetin (0, 10, 25, 75 and 100 μM). The inhibition reversibility of hesperetin againt XO was assessed through plotting reaction velocity against enzyme concentration.

The inhibition type of hesperetin on XO was determined by maintaining the concentration of XO at 0.04 U/mL and changing xanthine concentration from 0 to 500 μM. The reaction velocity was measured by adding various concentrations of hesperetin (0, 1, 2.5, 5, 7.5 and 10 μM). The double reciprocal Lineweaver-Burk plots were generated to evaluate hesperetin's potential inhibitory effect on XO by Equation (2):

$$\frac{1}{v} = \frac{K_m}{V_{max}}\left(1 + \frac{[I]}{K_i}\right) + \frac{1}{[S]} + \frac{1}{V_{max}}\left(1 + \frac{[I]}{\alpha K_i}\right) \quad (2)$$

The secondary plots from the Lineweaver-Burk curves were constructed using Equations (3) and (4):

$$\text{Slope} = \frac{K_m}{V_{max}} + \frac{K_m[I]}{V_{max}K_m} \quad (3)$$

$$\text{Y} - \text{intercept} = \frac{1}{V_{max}^{app}} = \frac{1}{V_{max}} + \frac{[I]}{\alpha K_i V_{max}} \quad (4) \quad (4)$$

Where V is the enzyme reaction velocity in the presence or absence of hesperetin. K_m and K_i refer to the Michaelis-Menten constant and inhibitory constant, respectively. V_{max} and V_{max}^{app} denote the maximum velocity of the enzymatic reaction and the apparent maximum velocity of the enzymatic reaction, respectively. The value of α represents the ratio of the uncompetitive inhibition constant to the competitive inhibition constant. If the value of α is 1, it is regarded as a non-competitive inhibition. *[I]* and *[S]* stand for the concentrations of inhibitor and substrate, respectively.

2.4. Antioxidant Activities of Hesperetin in Different Reaction Systems

2.4.1. 2,2-Diphenyl-1-Picrylhydrazyl (DPPH) Scavenging Activity

The DPPH scavenging assay was carried out using the method described by Tang et al. (2016) with slight modifications. Briefly, DPPH (100 μL, 0.1 mM) and hesperetin (100 μL, 0–50 μM) were mixed and incubated at room temperature for 30 min in the dark. Pure ethanol was used as the control. The absorbance of the mixture was recorded at 517 nm. The scavenging activity of hesperetin against DPPH radicals was expressed as IC_{50} value based on the decrease in absorbance.

2.4.2. O_2^- Scavenging Activity in PMS-NADH System

Through the PMS-NADH system, O_2^- is generated non-enzymatically, and it is widely used to assess the antioxidant activities of the UA inhibitors. Specifically, NBT (80 μL, 156 μM), NADH (75 μL, 780 μM) and hesperetin sample solution in different concentrations (5 μL, final concentration at 0–60 μM) were incubated at 25 °C for 10 min. The PMS solution (40 μL, 400 μM) was then added to

 doi:10.20944/preprints202404.1678.v1

initiate the reaction. The absorbance was measured every 30 s for 5 min at 560 nm. The O_2^- inhibition ratio was calculated from the proportional change in absorbance (Zhao et al., 2020).

2.4.3. O_2^- Scavenging Activity in XO Enzymatic Reaction

The O_2^- produced by XO can reduce NBT to a blue formazan exhibiting a characteristic absorbance at 560 nm (Masuoka et a., 2015). Briefly, XO (50 μL, 0.04 U/mL) was mixed with different concentrations of hesperetin (0, 1.0×10^{-6}, 2.0×10^{-6}, 3.0×10^{-6}, 4.0×10^{-6}, 5.0×10^{-6}, 6.0×10^{-6}, 7.0×10^{-6}, 8.0×10^{-6},10.0×10^{-6}, 15.0×10^{-6}, 20.0×10^{-6} mol/L) in 96-well plates and the mixtures were incubated for 30 min at 37 °C. Then, NBT (50 μL) and various concentrations of xanthine (50 μL) at 1.0×10^{-4}, 2.0×10^{-4} and 5.0×10^{-4} mol/L, respectively, was successively added into the solution to initiate the reaction. Blank controls were performed by replacing samples with phosphate-buffered saline (PBS) buffer (pH 7.4). The absorbance of the mixture was monitored at 560 nm for 5 min and the O_2^- scavenging activity of hesperetin in the reaction system was expressed as the relative inhibition ratio as determined by the increased velocity of the absorbance (Zhao et al., 2020).

2.5. Fourier Transform Infrared Spectra Measurements on XO

The FT-IR spectra measurements were performed according to Tang and Zhao (2019) with slight modifications. The spectra were monitored on a Vertex FT-IR spectrometer (Bruker Co., Karlsruhe, Germany) based on the attenuated total reflection infrared (ATR-IR) technique with the spectral range in 1800-1400 cm^{-1} employing a resolution of 0.16 cm^{-1} and 64 scans. The sample solution was prepared by mixing hesperetin (1 mM) and XO (2 U/mL) and incubated at 37 °C for 30 min. The spectra of PBS solution (pH 7.2) was used as a background spectrum and free compound were monitored over a wavenumber range of 1800-1400 cm^{-1}. A baseline subtraction, smoothing, second derivative analysis, deconvolution, and curve fitting of the amide I and II band were conducted on the collected spectrum data using Omnic Specta Software v7.2 (Nicolet Instrument Co., Madison, WI, USA).

2.6. Fluorescence Spectra Measurements on XO

The fluorescence spectra were performed on a spectrofluorometer (model F-7000, Hitachi, Japan) using a quartz cell with a path length of 1.0 cm and a circulating water bath. The measurements were carried out using an excitation wavelength at 280 nm, an emission wavelength of 300-500 nm, and a bandwidth at 8 nm for both excitation and emission at different temperatures (298, 304 and 310 K). The hesperetin solution was successively added into XO solution (0.1 U/mL), which was equilibrated thoroughly prior to measurement. The speactra of the blank PBS buffer was recorded and subtracted from the sample spectra to ensure that the sample spectra were accurate (Zhao et al., 2020).

To remove the inner filter and re-absorption, all the fluorescence data obtained were corrected by Equation (5):

$$F_c = F_m antilog \frac{A_{ex}+A_{em}}{2} \quad (5)$$

where F_c is the value obtained after correcting the measured fluorescence intensity and F_m is measured fluorescence intensity that is directly measured from the sample. A_{ex} and A_{em} represent the absorbance of hesperetin at the excitation and emission wavelengths, respectively.

2.7. Molecular Docking Studies

Molecular docking is used to verify the binding activity between an active ingredient and its ligand. AutoDock Vina v1.1.2 software (Scripps Research, La Jolla, CA, US) which operates with a semi-flexible docking method in a docking accuracy of up to 78%, was used as the molecular docking program in this study. The target crystal structure of XO (PDB: 1N5X) was downloaded from the RCSB Protein Data Bank (http://www.rcsb.org/pdb), and the structure of hesperetin was obtained from Pubchem (https://www.ncbi.nlm.nih.gov/pccompound). Autodock Tools were used to detect and assign rotatable bonds to ligands. This process involves removing all water molecules and

 doi:10.20944/preprints202404.1678.v1

ligands from the polypeptide chain, adding hydrogen atoms, adding Gasteiger charges, and repairing the missing and terminal residues. A grid box enclosing the entire binding site of XO was defined with dimensions of 126 Å × 126 Å × 126 Å and a grid spacing of 0.375 Å (Tang & Zhao, 2019). In addition, the reversible bond of the ligand selected by Autodock Tools was determined by the ligand in the small molecule hesperetin. The docking method exhibiting the lowest binding energy and highest percentage frequency was chosen to determine the conformation of the complex. A visible binding gesture was generated using PyMOL (https://sourceforge.net/projects/pymol/) as the output.

2.8. Statistical Analysis

The experiment was repeated in triplicate and the data were represented as mean ± standard deviation (n=3). One-way ANOVA was applied to detect differences in the data. A *p*-value <0.05 was considered significant. Graphpad Prism (version 9.0) software (GraphPad Software, San Diego, CA, USA) was used to analyse data.

3. Results and Discussion

3.1. Inhibitory Effect of Hesperetin on XO Activity

Both of allopurinol and hesperetin exhibited XO inhibition activities in a concentration-dependent manner (Figure 1). Allopurinol showed a significant inhibitory effect on XO with an IC_{50} value of 0.32 ± 0.01 μM while hesperetin also demonstrated a notable inhibitory effect, with the IC_{50} value being 6.97 ± 0.02 μM. Although its IC_{50} value is higher than that of allopurinol, hesperetin still shows significant potential as an effective natural suppressor of xanthine oxidase. Liu et al. (2016) and Roza et al. (2016) reported IC_{50} values for hesperetin at 16.48 μM and 16.69 μM, respectively, which were marginally higher than that recorded in this study. The variation might be due to discrepancies in experimental conditions, the purity of hesperetin, and the sensitivity of the assays employed in different investigations. It should be noted that despite this, hesperetin is identified as a potent inhibitor of XO with its desirable IC_{50} value in previous and current studies. This was due to the hydroxyl group at C-7 on aryl ring A of the flavonoid hesperetin leading to a strong inhibition activity of XO (Zeng et al., 2019). Furthermore, hesperetin demonstrated a more potent inhibitory effect on XO compared to its glycosylated derivative, hesperidin (de Souza et al., 2015; Liu et al., 2016). It has been noted that replacing the hydroxyl group at the C-7 position with a glycoside in the structure of dietary flavonoids like hesperidin significantly decreases XO inhibitory activity (de Souza et al., 2015; Liu et al., 2016). The addition of glycosyl groups to flavonoids may reduce their enzyme inhibitory effectiveness due to increased molecular size and restricted access to the enzyme's active site (Zhao et al., 2020).

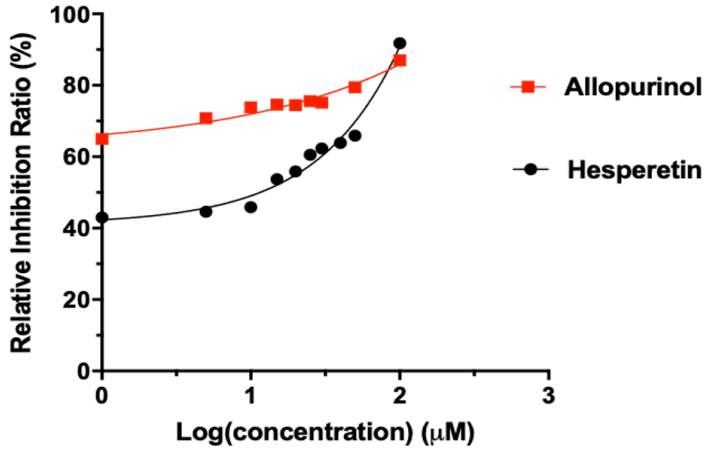

 doi:10.20944/preprints202404.1678.v1

Figure 1. Inhibitory effects of hesperetin and allopurinol on the activity of xanthine oxidase (XO, pH 7.4, 37 °C) with c(XO) = 0.04 U/mL and c(xanthine) = 0.5 mM. Each point represents the mean ± S.D. of triplicate measurements.

3.2. Reversibility and Inhibition Type of Hesperetin on XO

To assess the kinetic mechanism of hesperetin on inhibiting XO activity, velocity plots and Lineweaver-Burk plots were established. All straight lines decreased in slope as hesperetin concentration was increased, and they intersected at the origin (Figure 2A), suggesting that hesperetin act as an inhibitor by binding to the active site of XO while the effective concentration of the enzyme remain the same (Zeng et al., 2018). As shown in Figure 2B, the horizontal axis intercept ($-1/K_m$) grew with the increasing concentration of the inhibitor, indicating that hesperetin exerted a competitive inhibition effect (Yan et al., 2013). Hesperetin might compete with the xanthine substrate to occupy the enzyme's active site (Malik, Dhiman, & Khatkar, 2019). In addition, Lim (2019) demonstrated that hesperetin inhibited XO through a reversible and competitive mechanism. In this study, the inhibition constant (*Ki*) value was determined at $(2.15\pm0.05)\times10^{-6}$ mol/L, a slightly higher than that (1.92×10^{-6} mol/L) of allopurinol also belonging to the competitive type. Thus, hesperetin could have a greater affinity for XO, allowing it to bind XO readily and tightly (Tang & Zhao, 2019; Zeng et al., 2019).

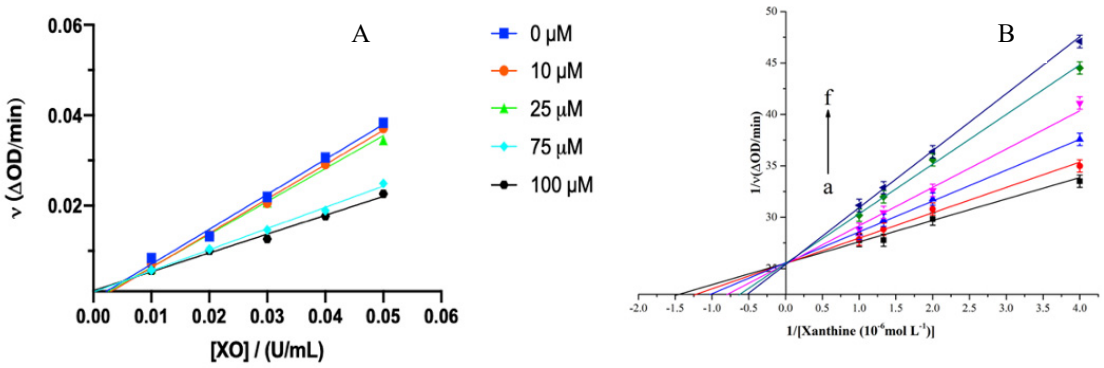

Figure 2. (A) Kinetic plots with c(XO) = 0.01, 0.02, 0.03, 0.04 and 0.05 U/ml, c(hesperetin) = 0, 10, 25, 75 and 100 μM, and c(xanthine) = 0.5 mM, respectively. (B) Lineweaver-Burk plots in the absence and presence of hesperetin on XO with c(xanthine) from 0 to 5.0×10^{-4} mol/L (0-500 μM), c(XO) = 0.04 U/ml and c(hesperetin) = 0, 1, 2.5, 5, 7.5 and 10 μmol/L for curve a-f, respectively. Each point in the figures represents the mean ± S.D. of triplicate measurements.

3.3. Scavenging Activities of Hesperetin on Radicals Generated in Different Reaction Systems

During the XO enzymatic reaction, xanthine is oxidized to UA along with ROS production. Xanthine and oxygen are simultaneously used as substrates following a ping-pong mechanism, under which the enzyme can transform into an intermediate state (Zhao et al., 2020). Subsequently, O_2 as another substrate is catalyzed by the oxidized intermediate of XO to generate the O_2^- radical or by reduced intermediate of XO (EII) to generate hydrogen peroxide (H_2O_2) (Zhang et al., 2016). The intermediates ultimately revert to the original form of XO and the reaction is completed (Zhu et al., 2021). Hence, the three pathways for inhibitors to suppress the production of O_2^- radicals can be categorized as follows: (I) Inhibitors block the formation of UA by inhibiting the XO reactions, thus preventing the generation of O_2^- radicals and H_2O_2; (II) Reductive inhibitors initiate the reduction reactions of XO, resulting in the reduced enzyme catalyzing only O_2 to release H_2O_2; (III) Inhibitors as antioxidants directly scavenge O_2^- radicals (Zhang et al., 2016). Therefore, superoxide anion generation can be inhibited by inhibiting the formation of UA, generating XO reduction reactions and scavenging O_2^- radicals.

 doi:10.20944/preprints202404.1678.v1

As seen in Figure 3A, hesperetin scavenged about 85.6% of DPPH radical at a concentration of 50 × 10^{-6} mol/L, suggesting that hesperetin exhibit a strong antioxidant character and have the capacity to reduce the XO molecule, possibly due to its ability to prevent the free radicals from penetrating into the acyl chain region of enzyme (Zhu et al., 2021). In contrast, although the O_2^- radical scavenging activity was gradually enhanced, it eventually remained constant under 50% at 53 × 10^{-6} mol/L (Figure 3A), indicating that hesperetin had lower O_2^- scavenging activity than DPPH one. The finding was consistent with the conclusion that hesperetin inhibited the formation of O_2^- radicals in a competitive manner when UA was suppressed (Zhang et al., 2020).

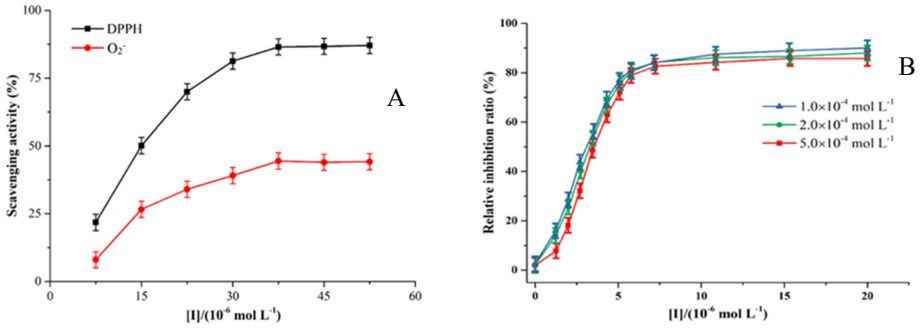

Figure 3. (A) DPPH and O_2^- radical scavenging capacity of hesperetin in non-enzymatic system. (B) Inhibition effects of hesperetin (0, 1.0×10^{-6}, 2.0×10^{-6}, 3.0×10^{-6}, 4.0×10^{-6}, 5.0×10^{-6}, 6.0×10^{-6}, 7.0×10^{-6}, 8.0×10^{-6},10.0×10^{-6}, 15.0×10^{-6}, 20.0×10^{-6} mol/L) on the O_2^- radical generated by XO at three different concentrations of xanthine (1.0×10^{-4}, 2.0×10^{-4} and 5.0×10^{-4} mol/L) with XO (0.04 U/mL).

At the concentration range of 2.0-5.0×10^{-6} mol/L, hesperetin rapidly inhibited the formation of O_2^- radicals in the enzymatic system and its relative inhibition ratio reaching around 90% (Figure 3B). Nevertheless, the inhibition effect of hesperetin on the O_2^- radicals generated by XO reaction did not vary much with a change in xanthine concentration, indicating that xanthine had a limited effect on the hesperetin's dose-response curve. According to these findings, hesperetin had a lower scavenging rate compared to its inhibitory rate against O_2^- radicals generated by the XO reaction system. The XO protein contains two separate substrate-binding sites, the Molybdenum (Mo) center, and the Flavin adenine dinucleotide (FAD) center. At the Mo center, xanthine is oxidized, while at the FAD center, oxygen is reduced with transferred electrons, generating O_2^- radicals or H_2O_2 (Masuoka et al., 2015). Therefore, the findings suggested that hesperetin bind to the Mo center of XO and prevent the entry of xanthine and the transfer of electrons. By inhibiting the generation of O_2^- radicals, hesperetin not only blocked the conversion of xanthine to UA but also the conversion of oxygen to ROS (Zhang et al., 2016).

3.4. FT-IR Spectra of XO Mediated by Hesperetin

FT-IR spectroscopy is an effective tool for determining conformational changes in the secondary structures of proteins (Zhao et al., 2020). According to Tang & Zhao (2019), proteins have nine characteristic vibrational bands or group frequencies that respond to conformational changes in their secondary structures. In particular, three characteristic vibrational bands of protein amide I, II, and III can be mainly interpreted from peaks of protein absorption in various wavenumber ranges, which are restricted to group frequency interpretations. Among them, amide I band (1700–1600 cm^{-1}, predominantly caused by C=O stretching vibrations) and amide II band (1600–1500 cm^{-1}, caused by C-N stretching coupled with N-H in-plane bending) are the two main vibrational bands of the peptide moiety associated with the secondary structure changes (Zhang et al., 2016). Additionally, amide I band is more commonly used than amide II band since the former has higher sensitivity and is more responsible for the modification of the protein secondary structure (Zhao et al., 2020). The spectral wavenumber ranges of 1615–1637 cm^{-1}, 1638–1648 cm^{-1}, 1649–1660 cm^{-1}, 1661–1680 cm^{-1} and

 doi:10.20944/preprints202404.1678.v1

1681–1692 cm^{-1} are most assigned to β-sheet, random coil, α-helix, β-turn and β-anti-parallel, respectively (Yan et al., 2013). As seen in Figure 4, the peak position of the amide I band of XO shifted from 1645 to 1648 cm^{-1} with the addition of hesperetin, whereas that of amide II band moved to a less extent from 1547 to 1543 cm^{-1}. There was no absorption of hesperetin within the specified spectra range, so the difference between the existence of hesperetin and the interaction could be ignored. These changes elucidated that hesperetin interacted with the C=O and C-N groups of the enzyme, resulting in a rearrangement of the carbonyl hydrogen bonding network (Zhang et al., 2016).

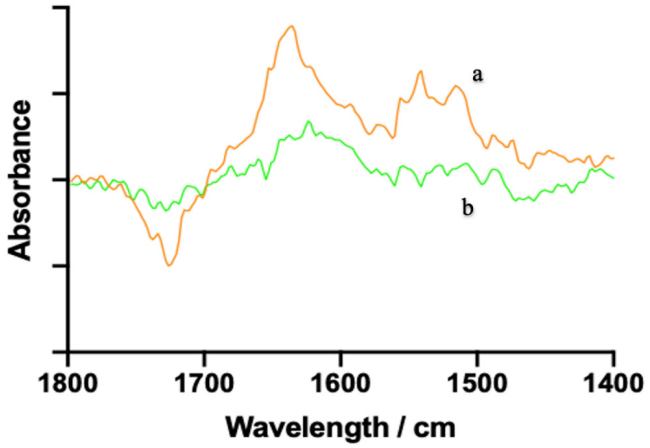

Figure 4. The FT-IR spectra of (a) hesperetin– xanthine oxidase (XO) complex and (b) free XO solution in the region of 1800–1400 cm^{-1} at pH 7.2, 37 °C for 30 min with c(XO) = 2.0 U/mL and c(hesperetin) = 1.0×10^{-3} mol/L.

3.5. Fluorescence Quenching of XO Induced by Hesperetin

As discussed above, hesperetin exhibited remarkable inhibitory activity against XO, suggesting hesperetin's capacity of binding directly to the enzyme. To further investigate the interaction mechanism between hesperetin and XO, the fluorescence assay was conducted to gain additional insight into the interaction process, including binding constant and binding site.

In general, XO consists of three types of light-emitting groups, namely tryptophan, tyrosine, and phenylalanine (Zhao et al., 2020). The fluorescence quenching spectra of XO affected by hesperetin is depicted in Figure 5. Two peaks of fluorescence emission were observed at 340 and 405 nm, while hesperetin did not show intrinsic fluorescence in the assay (shown as the curve m). The fluorescence emission peak at 340 nm was chosen for further analysis of the collected data due to its distinct intensity change. It was found that the fluorescence intensity (curves from a to k) at 340 nm was significantly decreased with the increasing concentration of hesperetin from 0 to 20 μM. The fluorescence quenching ratio reflecting the quenching strength of intrinsic fluorescence intensity of XO by the inhibitor was calculated to be 68.05%. Moreover, the maximum emission wavelength presented a slight red shift from 340 nm to around 352 nm, indicating that the microenvironment around chromophores in XO was altered during the interaction (Zhao et al., 2020). The results revealed that hesperetin could interact with the XO enzyme and exert a strong fluorescence quenching effect.

 doi:10.20944/preprints202404.1678.v1

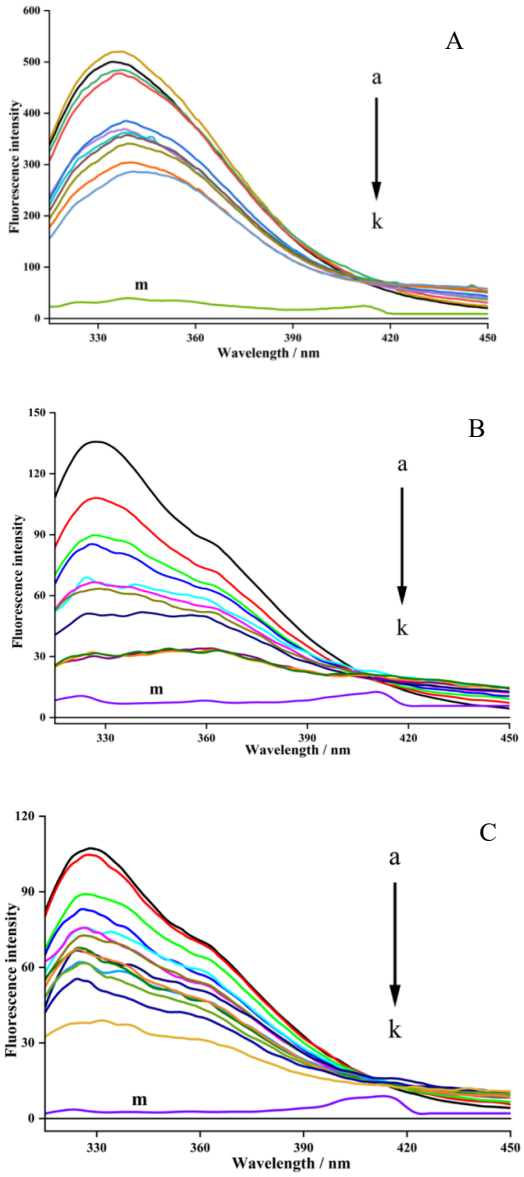

Figure 5. Fluorescence spectra of xanthine oxidase (XO) in the presence of hesperetin at different concentrations from 0, 2, 4, 6, 8, 10, 12, 14, 16, 18 and 20 μM, respectively for curves a → k with c(XO) = 0.1 U/mL at 298 K (A), 304 K (B) and 310 K (C) respectively (λex = 280 nm, λem = 340 nm, pH = 7.2).

3.6. Molecular Docking Results

The molecular docking method has been widely used to simulate the potential binding mode of ligands and proteins based on the "lock" and "key" principle (Zhao et al., 2020). The binding energy of conformational clusters is categorized according to the number of energy through cluster analysis using a root-mean-square deviation (rmsd) tolerance of 2.0 Å. It was found that the predicted average binding energy ($\Delta G_{binding}$ = intermolecular energy + torsional energy) for the compound hesperetin was -10.9 kcal/mol. Furthermore, the binding energy determined for hesperetin to XO was found to be -10.9 kcal/mol. This result aligns with the anticipated inhibitory action of hesperetin against XO as predicted in the study by Zhao et al. (2020). Since the binding energy of hesperetin to XO is less than 0, they can bind spontaneously. More importantly, an active ingredient has a strong affinity to the

 doi:10.20944/preprints202404.1678.v1

target when its binding energy is less than -5.0 kcal/mol (Liu et al., 2016). Therefore, the compound hesperetin is highly affinity to the protein XO.

Furthermore, the ligand molecule hesperetin was surrounded with residues Glu402, Gly399, Lys249, Glu267, Thr354 and Ile264 of XO within 4 Å (Figure 6A). There were five hydrogen bonds formed for the compound hesperetin with Ile264 (3.5 Å), Lys249 (3.0 Å), Gly399 (2.6 Å) and Thr354 (3.2 Å). As shown in Figure 6B, the compound hesperetin was also found adjacent to several hydrophobic residues (Leu257, Arg394, Val259, Ser347, Gly350 and Thr 262) in the active pocket of XO, suggesting the presence of hydrophobic interactions between hesperetin and XO. The two-dimensional map of the docking simulation provided evidence that the ligand molecule hesperetin could bind to XO through hydrogen bonds and hydrophobic forces, which stabilized the binding conformation of the hesperetin-XO complex. Another study conducted by Malik et al. (2019) revealed that new derivatives of hesperitin such as methylated hesperitin and estered hesperitin interacted with amino acid residues of Ser1080, Phe798, Gln1194, Arg912, Thr1083, Ala1078 and Met1038, which were found to be located in the active cavity of XO.

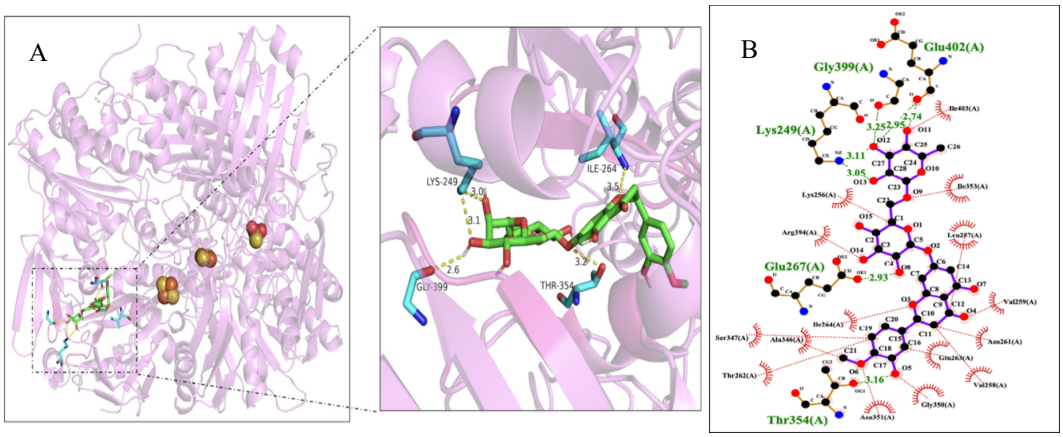

Figure 6. (A) Molecular docking results of hesperetin with XO. Key residues are demonstrated as stick models and hydrogen bonds are labeled as yellow dashed lines with distance of Å. (B) An analysis of the interactions between hesperetin and hydrophobic and hydrophilic amino acids around the active site of XO. Hydrophobic amino acids are labeled as red semicircles while hydrophilic amino acids are labeled as green characters.

According to the molecular docking results, it could be deduced that hesperetin was inserted into the active center of the molybdopterin (Mo-pt) cofactor domain of XO in a competitive manner, inhibiting the entry of its substrate into the active center and the enzyme-catalyzed reaction (Enroth et al., 2000). If the concentration of hesperetin was relatively low, UA synthesis would be slightly impaired (Tang & Zhao, 2019). On the contrary, in the presence of enhanced concentrations of hesperetin, the enzyme was remarkably altered, preventing its substrate from entering the active site of XO (Mo-pt), and then inhibiting the formation of UA (Tang & Zhao, 2019). A moderate inhibition of the generation of superoxide anion was therefore observed. With the increase of hesperetin concentration, its ability to inhibit the formation of UA and prevent the electrons transfer to the FAD center greatly increased, resulting in a strong inhibition of superoxide anion formation. These results supported the inhibition mechanism of hesperetin against XO activity through its inhibiting UA formation and superoxide anion production.

4. Conclusion

Hesperetin exhibited a notable inhibitory activity against XO with an IC_{50} value of 6.97 ± 0.02 μM. Hesperetin inhibited the formation of superoxide anion by inhibiting UA production and suppressing oxygen reduction. The XO activity could be significantly inhibited by hesperetin's binding to the enzyme, occupying the catalytic center (Mo-pt domain), interfering with substrate

 doi:10.20944/preprints202404.1678.v1

entry, altering the conformational state in its secondary structures. In light of its prominent antioxidant properties against ROS and the interaction with XO, hesperetin has the potential of being developed as an innovative XOI agent or a functional food supplement to treat hyperuricemia. Further in vivo research is warranted to confirm hesperetin's potential as a substitute for treating hyperuricemia.

Author Contributions: Yinying Liu: Data curation, Investigation, Methodology, Software, Visualization, Writing – original draft. **Qianqian Chen:** Formal analysis, Methodology, Validation. **Hanyu Lu:** Software, Visualization, Writing – original draft. **Zhongxiang Fang:** Supervision, Resources, Writing – review & editing. **Shengmin Lu:** Conceptualization, Supervision, Funding acquisition, Project administration, Resources, Writing – review & editing.

Acknowledgments: This work was financially supported by the Key Research and Development Project (2017C02004) of Science and Technology Department of Zhejiang Province, China.

Conflicts of Interest: The authors declare no conflict of interest.

References

1. An, M.-F., Shen, C., Zhang, S.-S., Wang, M.-Y., Sun, Z.-R., Fan, M.-S., Zhang, L.-J., Zhao, Y.-L., Sheng, J., & Wang, X.-J. (2023). Anti-hyperuricemia effect of hesperetin is mediated by inhibiting the activity of xanthine oxidase and promoting excretion of uric acid. *Frontiers in Pharmacology*, *14*, 1128699. https://doi.org/10.3389/fphar.2023.1128699
2. Bao, R., Chen, Q., Li, Z., Wang, D., Wu, Y., Liu, M., Zhang, Y., & Wang, T. (2022). Eurycomanol alleviates hyperuricemia by promoting uric acid excretion and reducing purine synthesis. *Phytomedicine*, *96*, 153850. https://doi.org/10.1016/j.phymed.2021.153850
3. Cao, L., Ma, B., Yi, B., Liu, Y., & Sun, J. (2023). Discovery of natural multitarget xanthine oxidase inhibitors for therapeutic hyperuricemia using virtual screening, network pharmacology and in vitro experimental verification. *Chemistry Select*, *8*(30), e202301939. https://doi.org/10.1002/slct.202301939
4. Chen, N., Wang, R., Li, H., Wang, W., Wang, L., Yin, X., Yao, R., & Yang, B. (2022). Flavonoid extract of saffron by-product alleviates hyperuricemia via inhibiting xanthine oxidase and modulating gut microbiota. *Phytotherapy Research*, *36*(12), 4604–4619. https://doi.org/10.1002/ptr.7579
5. Cheng-yuan, W., & Jian-gang, D. (2023). Research progress on the prevention and treatment of hyperuricemia by medicinal and edible plants and its bioactive components. *Frontiers in Nutrition*, *10*, 1186161. https://doi.org/10.3389/fnut.2023.1186161
6. de Souza, V. T., de Franco, É. P., de Araújo, M. E., Messias, M. C., Priviero, F. B., Frankland Sawaya, A. C., & de Oliveira Carvalho, P. (2015). Characterization of the antioxidant activity of aglycone and glycosylated derivatives of hesperetin: An in vitro and in vivo study. *Journal of Molecular Recognition*, *29*(2), 80–87. https://doi.org/10.1002/jmr.2509
7. Dong, X., Wang, B., Cao, J., Zheng, H., & Ye, L. (2021). Ligand fishing based on bioaffinity ultrafiltration for screening xanthine oxidase inhibitors from citrus plants. *Journal of Separation Science*, *44*(7), 1353–1360. https://doi.org/10.1002/jssc.202000708
8. Dório, M., Benseñor, I. M., Lotufo, P., Santos, I. S., & Fuller, R. (2022). Reference range of serum uric acid and prevalence of hyperuricemia: A cross-sectional study from baseline data of Elsa-Brasil cohort. *Advances in Rheumatology*, *62*(1), 15-25. https://doi.org/10.1186/s42358-022-00246-3
9. Enroth, C., Eger, B., Okamoto, K., Nishino, T., Nishino, T., & Pai, E. (2000). Crystal structures of bovine milk xanthine dehydrogenase and xanthine oxidase: Structure-based mechanism of conversion. *Proceedings of The National Academy of Sciences*, *97*(20), 10723-10728. https://doi.org/10.1073/pnas.97.20.10723
10. Haidari, F., Ali Keshavarz, S., Reza Rashidi, M., & Mohammad Shahi, M. (2009). Orange juice and hesperetin supplementation to Hyperuricemic rats alter oxidative stress markers and xanthine oxidoreductase activity. *Journal of Clinical Biochemistry & Nutrition*, *45*(3), 285-291. https://doi.org/10.3164/jcbn.09-15
11. Haidari, F., Rashidi, M. R., & Mohammad-Shahi, M. (2012). Effects of orange juice and hesperetin on serum paraoxonase activity and lipid profile in hyperuricemic rats. *BioImpacts*, *2*(1), 39–45. https://doi.org.10.5681/bi.2012.005
12. Hou, Y., & Jiang, J. G. (2013). Origin and concept of medicine food homology and its application in modern Functional Foods. *Food & Function*, *4*(12), 1727-1741. https://doi.org/10.1039/c3fo60295h
13. Lim, S. L. (2019). Interaction of apigenin and hesperetin on xanthine oxidase inhibition and their inhibitory mechanism (Doctoral dissertation, Tunku Abdul Rahman University College).

 doi:10.20944/preprints202404.1678.v1

14. Liu, K., Wang, W., Guo, B., Gao, H., Liu, Y., Liu, X., Yao, H., & Cheng, K. (2016). Chemical evidence for potent xanthine oxidase inhibitory activity of ethyl acetate extract of *Citrus aurantium* L. dried immature fruits. *Molecules*, *21*, 302 https://doi.org/10.3390/molecules21030302
15. Masuoka, N., Nihei, K., Maeta, A., Yamagiwa, Y., & Kubo, I. (2015). Inhibitory effects of cardols and related compounds on superoxide anion generation by xanthine oxidase. *Food Chemistry*, *166*, 270-274. https://doi.org/10.1016/j.foodchem.2014.06.021
16. Malik, N., Dhiman, P., & Khatkar, A. (2019). In silico design and synthesis of hesperitin derivatives as new xanthine oxidase inhibitors. *BMC Chemistry*, *13*, 53. https://doi.org/10.1186/s13065-019-0571-1
17. Roohbakhsh, A., Parhiz, H., Soltani, F., Rezaee, R., & Iranshahi, M. (2015). Molecular mechanisms behind the biological effects of Hesperidin and Hesperetin for the prevention of cancer and cardiovascular diseases. *Life Sciences*, *124*, 64–74. https://doi.org/10.1016/j.lfs.2014.12.030
18. Roza, O., Martins, A., Hohmann, J., Lai, W. C., Eloff, J., Chang, F. R., & Csupor, D. (2016). Flavonoids from Cyclopia genistoides and their xanthine oxidase inhibitory activity. *Planta Medica*, *82*(14), 1274–1278. https://doi.org/10.1055/s-0042-110656
19. Tang, H., & Zhao, D. (2019). Investigation of the interaction between salvianolic acid C and xanthine oxidase: Insights from experimental studies merging with molecular docking methods. *Bioorganic Chemistry, 88*, 1-10. https://doi.org/10.1016/j.bioorg.2019.102981
20. Tang, W., Lin, L., Xie, J., Wang, Z., Wang, H., Dong, Y., Shen, M., & Xie, M. (2016). Effect of ultrasonic treatment on the physicochemical properties and antioxidant activities of polysaccharide from *Cyclocarya paliurus*. *Carbohydrate Polymers, 151,* 305-312. https://doi.org/10.1016/j.carbpol.2016.05.078
21. Wu, D., Chen, R., Zhang, W., Lai, X., Sun, L., Li, Q., Zhang, Z., Cao, J., Wen, S., Lai, Z., Li, Z., Cao, F., & Sun, S. (2022). Tea and its components reduce the production of uric acid by inhibiting xanthine oxidase. *Food & Nutrition Research*, *66*, 8239. https://doi.org/10.29219/fnr.v66.8239
22. Yan, J., Zhang, G., Hu, Y., & Ma, Y. (2013). Effect of luteolin on xanthine oxidase: Inhibition kinetics and interaction mechanism merging with docking simulation. *Food Chemistry*, *141*(4), 3766-3773. https://doi.org/10.1016/j.foodchem.2013.06.092
23. Zare, M., Sarkati, M. N., & Rahaiee, S. (2021). Fabrication of nanoparticles based on hesperidin-loaded chitosan-functionalized Fe_3O_4: Evaluation of in vitro antioxidant and anticancer properties. *Macromolecular Research*, *29*(11), 785–790. https://doi.org/10.1007/s13233-021-9091-7
24. Zeng, N., Zhang, G., Hu, X., Pan, J., & Gong, D. (2019). Mechanism of fisetin suppressing superoxide anion and xanthine oxidase activity. *Journal of Functional Foods*, *58*, 1-10. https://doi.org/10.1016/j.jff.2019.04.044
25. Zeng, N., Zhang, G., Hu, X., Pan, J., Zhou, Z., & Gong, D. (2018). Inhibition mechanism of baicalein and baicalin on xanthine oxidase and their synergistic effect with allopurinol. *Journal of Functional Foods*, *50*, 172-182. https://doi.org/10.1016/j.jff.2018.10.005
26. Zhang, C., Zhang, G., Pan, J., & Gong, D. (2016). Galangin competitively inhibits xanthine oxidase by a ping-pong mechanism. *Food Research International*, *89*(1), 152-160. https://doi.org/10.1016/j.foodres.2016.07.021
27. Zhao, J., Huang, L., Sun, C., Zhao, D., & Tang, H. (2020). Studies on the structure-activity relationship and interaction mechanism of flavonoids and xanthine oxidase through enzyme kinetics, spectroscopy methods and molecular simulations. *Food Chemistry*, *323*, 126807. https://doi.org/10.1016/j.foodchem.2020.126807
28. Zhou, Q., Su, J., Zhou, T., Tian, J., & Chen, J. (2017). A study comparing the safety and efficacy of febuxostat, allopurinol, and benzbromarone in Chinese gout patients: A retrospective cohort study. *International Journal of Clinical Pharmacology and Therapeutics*, *55*(02), 163–168. https://doi.org/10.5414/cp202629
29. Zhu, M., Pan, J., Hu, X., & Zhang, G. (2021). Epicatechin gallate as xanthine oxidase inhibitor: Inhibitory kinetics, binding characteristics, synergistic inhibition, and action mechanism. *Foods*, *10*(9), 2191. https://doi.org/10.3390/foods10092191